J Plant Growth Regul (2011) 30:185–198
DOI 10.1007/s00344-010-9183-7

Micromorpho-Anatomical Examination of 2,4-D Phytotoxicity in Grapevine (*Vitis vinifera* L.) Leaves

B. R. Bondada

Received: 13 July 2010 / Accepted: 16 September 2010 / Published online: 9 December 2010

Abstract The anatomical and micro-morphological alterations as induced by the auxinic herbicide, 2,4-D (2,4-dichlorophenoxy acetic acid) have not yet been elucidated for a commercially important fruit crop such as grapevine despite its super sensitivity to 2,4-D. Light and scanning electron microscopy techniques were employed to examine 2,4-D induced internal and external structural abnormalities in Merlot grapevines (*Vitis vinifera* L.). Healthy leaves were dorsiventrally flattened with well developed patterns of cellular structure and composition involving adaxial palisade parenchyma and abaxial spongy mesophyll. Dorsiventral variations in epidermal features involved large epidermal cells on the adaxial surface, and trichomes and stomata with turgid elliptical guard cells on the abaxial surface. The 2,4-D injured leaves were small and enated; the veins were fasciated with rugose bands of lamina existing between fasciated veins. The epidermal cells aggregated instead of being positioned coplanar to the epidermal plane. The adaxial elongated palisade parenchyma cells were transformed into an ovoid shape with intercellular spaces. An extensive development of replacement tissues took place on the abaxial surface wherein the stomata became roundish and were either raised or sunken with collapsed and cracked guard cells that developed abnormal outer stomatal ledges. These abnormalities are expected to severely perturb the vital functions of photosynthesis and transpiration ultimately leading to vine death attributable, at least in part, to the injured leaves.

B. R. Bondada (✉)
Washington State University Tri-Cities, 2710 University Drive, Richland, WA 99354, USA
e-mail: bbondada@wsu.edu

Keywords 2,4-D (2,4-Dichlorophenoxyacetic Acid) · Fasciation · Grapevine · Herbicide injury · Mesophyll · Stomata · Vein

Introduction

Grapevines (*Vitis vinifera* L.) are a broad-leaved perennial crop with a dicotyledonous and deciduous growth habit propagated vegetatively around the world for its fleshy fruit, the grape berry, which is used for making juice, distilled liquor and wine, and for consuming as fresh and dried fruit. Of all these products, wine enjoys the highest economic value and cultural significance on a global scale (Mullins and others 1998). The foliage leaves, the principle lateral organs of the grapevine shoot system constitute the basic building blocks of grape production for winemaking as they contribute to the ripening of grape berries through their morpho-anatomical relationships with photosynthesis (Pratt 1974; Bondada and others 2006). As the vine's most exposed organ, yet with no major protective structures found in other parts of the vine, they are the most sensitive vegetative structures of the grapevine. In light of their vulnerability to biotic and abiotic forces, grape growers exert significant time and effort to maintain healthy leaves throughout the growing season employing numerous cultural practices. Notwithstanding such preventive measures, vines develop abnormal and malformed leaves and this occurs frequently due to phytotoxicity of vapors and spray drifts of phenoxy herbicides (Kasimatis and others 1968; Bhatti and others 1996; Bondada and others 2006). As many as 100 or more herbicide formulations have been known to contain a phenoxy-type active ingredient and among them, one of the most commonly used phenoxy products is 2,4-D (2,4-dichlorophenoxy-acetic acid)

(Fig. 1), which is a synthetic auxin (Grossmann 2000). It is made up of a halogenated phenoxy compound containing two chlorine atoms substituted at the 2 and 4 positions and having an acetic acid side chain (Teixeira and others 2007). In popular usage; however, the symbol "2,4-D" (Fig. 1) has been used to mean any preparation that contains 2,4-dichlorophenoxy-acetic acid or any of its salts, amides, esters or related compounds (Tukey 1947).

Phytotoxic effects of 2,4-D to grapevine leaves from spray drift occurs every year (Al-Khatib and others 1991; Bondada and others 2006). As low as 3 ppm has been shown to cause injury to grapevines indicating their super sensitivity to 2,4-D (Kasimatis and others 1968; Bondada and others 2006). However, the extent of injury depends upon the climate and proximity to cereal fields where 2,4-D is sprayed to control broad-leaved weeds. For instance, it is of great concern in Midwest states of the US where 2,4-D is routinely used in row crops and most of the vineyards are adjacent to cereal fields (Skirvin 2008). Once 2,4-D has drifted to vineyards, grapevine leaves readily absorb and translocate the particles and volatiles of 2,4-D due to its selectivity against broad-leaved plants (Bhatti and others 1996). Following absorption, the shoots develop grotesque and malformed leaves, both young and old ones affecting their functions (Bondada and others 2006). Injury had been observed both in leaves that absorbed 2,4-D and sink organs (developing leaves, meristems, and so on) (Weintraub 1953; Hallam and Sargent 1970).

It is well known that herbicides absorbed from spray drift induce abnormal growth through morphological, anatomical, and cytological effects, which vary depending upon the type of the herbicide and plant species (Teixeira and others 2007). For instance, in soybean leaves, the non-auxinic herbicide, trifluralin caused palisade cells to be compact, short, and separated (Kust and Struckmeyer 1971) whereas glyphosate inhibited formation of intercellular air spaces in *Eucalyptus* leaves (Santos and others 2009). In contrast, the auxinic herbicide, 2,4-D induced elongation of mesophyll cells in grass leaves (Eames 1949) and injured membrane systems of the mesophyll cells in *Phaseolous vulgaris* (Loustalot and Muzik 1953). Although the injury to grapevine leaves ensuing from spray drifts of 2,4-D has been well documented in the literature (Kasimatis and others 1968; Al-Khatib and others 1991), the phytotoxic alterations in the internal organization of cells leading to deformed leaves remain elusive. Documenting injury to crops of commercial importance and yield loss from auxinic herbicides typically involves describing plant symptoms, their extent in the field and analyzing the symptoms at the morphological and cellular levels (Sciumbato and others 2004). This type of injury analysis is often achieved by physical or optical sectioning and scanning electron microscopic observations of tissues (Horiguchi and others 2006). Therefore, studies were conducted to elucidate the anatomical and micro-morphological characteristics of 2,4-D phytotoxicity to grapevine using light and scanning electron microscopy.

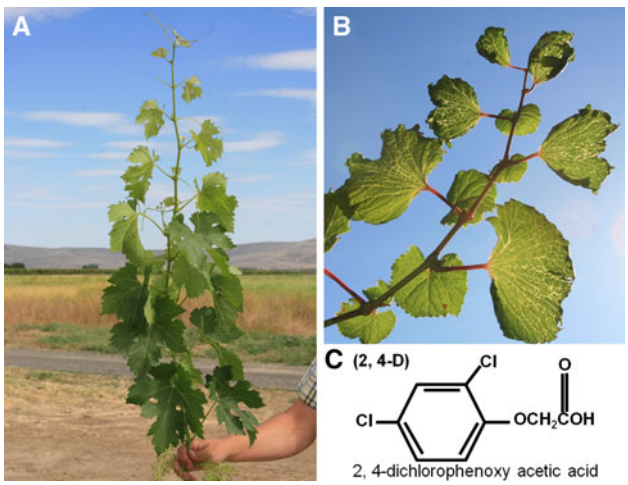

Fig. 1 Photographs of **a** healthy Merlot shoot, **b** 2,4-D injured shoot, and **c** structure of 2,4-D

Materials and Methods

Plant Material

Mature grapevines (*Vitis vinifera* L.) of the cultivar Merlot from a commercial vineyard were used with vine by row spacing of 1.83 m by 2.74 m on a uniformly deep (>1 m) loamy fine sand for examining the symptoms, anatomy and morphology of leaves injured by 2,4-D drift. The rows were oriented north–south. Vines were trained to two trunks and a bilateral cordon, which entailed training the vines in both directions along the cordon (an extension of the trunk) wire from the trunk. The shoots emerging from the cordon were positioned vertically using catch wires. Vines were spur-pruned during winter, that is, canes (a mature woody and lignified stem from previous season's shoot) were cut back to two count nodes/buds (the readily visible buds on a dormant cane, not including the small base buds); the noncount shoots (shoots arising from base buds of the spur) were removed at the beginning of bloom that approximately equated to 20 shoots/meter. Standard cultural practices were adopted to maintain healthy vines. This vineyard was chosen as it consistently develops phytotoxicity symptoms from 2,4-D drift year after year. The grapevines were monitored for 2,4-D phytotoxicity early in the season (May–June); once shoots displayed typical symptoms of 2,4-D injury (Bondada and others 2006), they were cut using a pruner and immediately brought to the laboratory with the cut end immersed in a

flask filled with water. Healthy shoots from a nearby block not affected by 2,4-D drift were also collected in a similar manner for comparison. The symptoms of 2,4-D injury on whole shoots and severed leaves were photographed using a digital camera (Canon, USA).

Light Microscopy

For light microscopy, thin sections of healthy and 2,4-D injured leaves were cut with a glass knife from epoxy-embedded tissue blocks, which were prepared by removing small pieces of leaf tissues. These tissues were fixed in 3% glutraldehyde overnight, washed with 0.1 M potassium phosphate buffer at pH 7.2 and post fixed in 2% osmium tetroxide overnight. The leaf tissues were then dehydrated in an acetone series and embedded in epoxy resin. From these blocks, thin sections with a glass knife were cut, placed on glass slides coated with Haupt's adhesive and stained with 1% toluidine blue. Slides were placed under an Axioskop 2 plus compound microscope (Carl Zeiss Inc., Thornwood, NY, USA) attached to a DXM 1200C digital camera (Nikon Instruments Inc., Melville, NY, USA), which was used for capturing digital images. The scale bars were calculated using a stage micrometer. Images of a stage micrometer and light micrographs using different objectives (4×, 10×, 20× and 40×) were taken and prints of scale bars and micrographs at the same magnification were used to place a scale line of known length in each micrograph.

Scanning Electron Microscopy (SEM)

Tissue samples from healthy and injured leaves were cut using a razor blade, fixed in 3% glutaraldehyde overnight, washed with 0.1 M potassium phosphate buffer at pH 7.2, and post-fixed in 2% osmium tetroxide overnight. The leaf samples were then dehydrated in a graded ethanol series and held in 95% ethanol for 2 h. The tissue samples were subsequently critical point-dried, coated with gold and viewed with a Hitachi S-570 scanning electron microscope (Hitachi Scientific Instruments, Mountain View, CA, USA) using an accelerated voltage of 15 kV. Before using the SEM, the scope magnification was calibrated by photographing a gold grid, and compared with a standard. The spot size was set towards the maximum diameter and minimum beam intensity with a standard working distance of 8 mm.

Results

Terminology to illustrate healthy leaf morpho-anatomical characteristics followed those of typical dicot leaves referred to by plant anatomists whereas the abnormal characteristics caused by 2,4-D injury used terms that best fit the description. Healthy leaves were petiolated with cuneiform lamina (Fig. 1a). The adaxial surface was astomatous and glabrous (Fig. 2a). On the contrary, the abaxial surface accommodated the epidermal outgrowths consisting of covering and filamentous trichomes (Fig. 2b, c). The covering trichomes were elongated, needle-like and single-armed (Fig. 2b). These trichomes occurred mostly on the minor veins. In addition to these types, abaxial surfaces had domatia, which are tufts of hairs found at the junctions (vein axils, intercostals regions—between veins) of primary and secondary veins (Fig. 2c). These hairs in the vein axils were of variable length but longer than the hairs on the smaller veins (Fig. 2c). The epicuticular wax morphology on both surfaces had a flat crystalloid structure with a high density of small interconnected platelets scattered parallel to the periclinal walls of the epidermal surface (Fig. 2d).

Grapevine leaves are hypostomatous, wherein, only on the abaxial surface are the closely packed epidermal cells interrupted by stomata (Fig. 2e). Stomata connecting the spongy mesophyll cells to the external environment were lenticular (crescent-shaped with relatively blunt ends) and consisted of two symmetrically opposed elliptical guard cells flanking an aperture (pore) arranged coplanar to the epidermal surface (Fig. 2e). Protuberances or ledges of elevated wall material facing the atmosphere known as outer stomatal ledges or rims rose from the guard cell surface like an incompletely roofed dome (Fig. 2e). In transverse sectional view, the two guard cells were seen as two rounded thick-walled cells with stomatal ledges appearing as archways or horns extended over the stomatal pore (Fig. 2f). Similar but reduced inner stomatal ledges projected towards one another (Fig. 2b). The outer ledges delimited the front (outer) cavity (forechamber) above the aperture and the inner ledge delimited the back (inner) cavity (rear chamber) which abutted the substomatal cavity (chamber) (Fig. 2f). Thus, with two pairs of stomatal ledges, the grapevine stomata had three apertures, an outer and inner aperture formed by the ledges and a central aperture about midway between the other two formed by the opposing guard cell walls. The guard cells had unevenly thickened walls with the dorsal wall (wall away from the pore) being thinner and therefore more flexible than the ventral wall (wall bordering the pore) (Fig. 2f).

Both the adaxial and abaxial epidermises were composed of a single layer of interlocked cells that were closely packed forming a continuous compact layer (Figs. 2a, 3a). Both the adaxial and abaxial epidermises were uniseriate; however, they were rather dissimilar in shape and size. The adaxial cells were bigger and relatively protruding due to increased height and lessened elongation rendering them

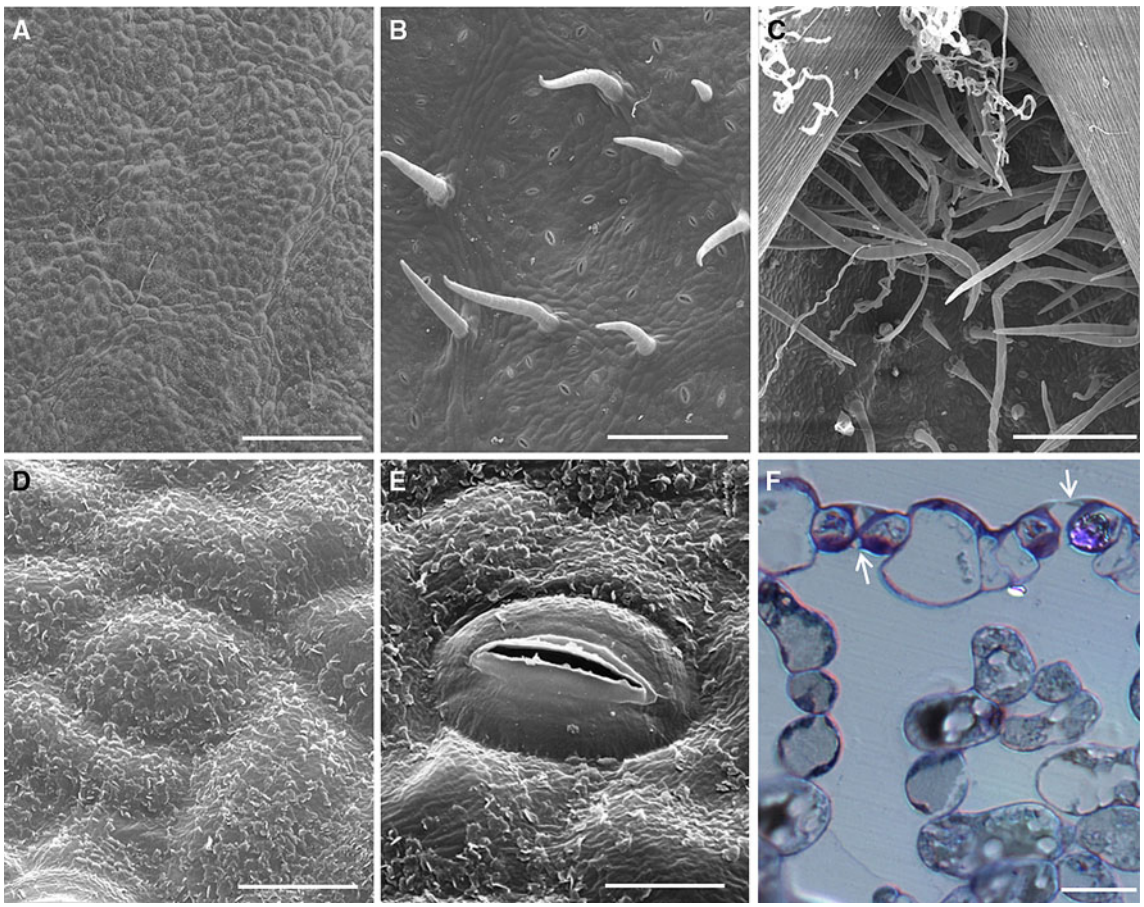

Fig. 2 Scanning electron micrographs of **a** adaxial epidermal cells of healthy leaf (*scale bar*: 250 μm), **b** abaxial trichomes and stomata of healthy leaf (*scale bar*: 176 μm), **c** domatia in the intercostal region (*scale bar*: 0.38 mm), **d** epicuticular wax as platelets (*scale bar*: 15 μm), **e** stoma of a healthy leaf (*scale bar*: 12 μm) and **f** light micrograph of stomata showing guard cells and cuticular ledges (*arrows*) (*scale bar*: 10 μm)

thicker (that is, deeper periclinally) than the abaxial cells (Fig. 3a). Both epidermises had cells of varying dimensions; however, the abaxial epidermis exhibited greater irregularity of cell form and size than the adaxial epidermis (Fig. 3a). In cross sections, they both appeared tabular in form, with thickened outer walls reinforced by the cuticular coverings and the conjunction of box-form cells (Fig. 3a). The outer periclinal walls of both epidermises were thicker than the inner periclinal walls. The outer walls were raised and convex, the inward facing cell walls adjoining the periclinal walls of mesophyll cells were also convex but had wavy indentations against which the individual mesophyll cells were pressed (Fig. 3a). As opposed to mesophyll cells, the epidermal cells (except stomata guard cells) had no chloroplasts (Fig. 3a). The side walls were relatively narrow (Fig. 3a).

Light microscopy revealed that healthy lamina had the distinct and characteristic organization of an angiosperm leaf (Fig. 3). The leaves were bifacial or dorsiventral in which the nonvascular mesophyll, comprising of parenchymatous tissues, was enclosed within the adaxial and abaxial epidermises (Fig. 3). The mesophyll tissue was well-differentiated into two types of parenchyma cells: palisade parenchyma and spongy parenchyma, both amply supplied with chloroplasts (Fig. 3a). However, the palisade parenchyma cells had more chloroplasts than the spongy mesophyll cells (Fig. 3a). Palisade parenchyma, so called because of its resemblance to a palisade (row of stakes) existed as a single layer of evenly spaced unbranched columnar cells arranged in a row and elongated at right angles to immediately below the adaxial surface (Fig. 3a). The palisade parenchyma cells contacted the adaxial epidermis in the same way that bristles contact the back of a brush (Fig. 3a). Below the palisade parenchyma, a porous spongy parenchyma developed consisting of five or six layers of variously shaped cells with a very extensive system of schizogenously-developed intercellular air spaces and connecting with the outer air through the stomata (Fig. 3a). Because of the presence of intercellular spaces, a considerable area of the mesophyll cell wall was

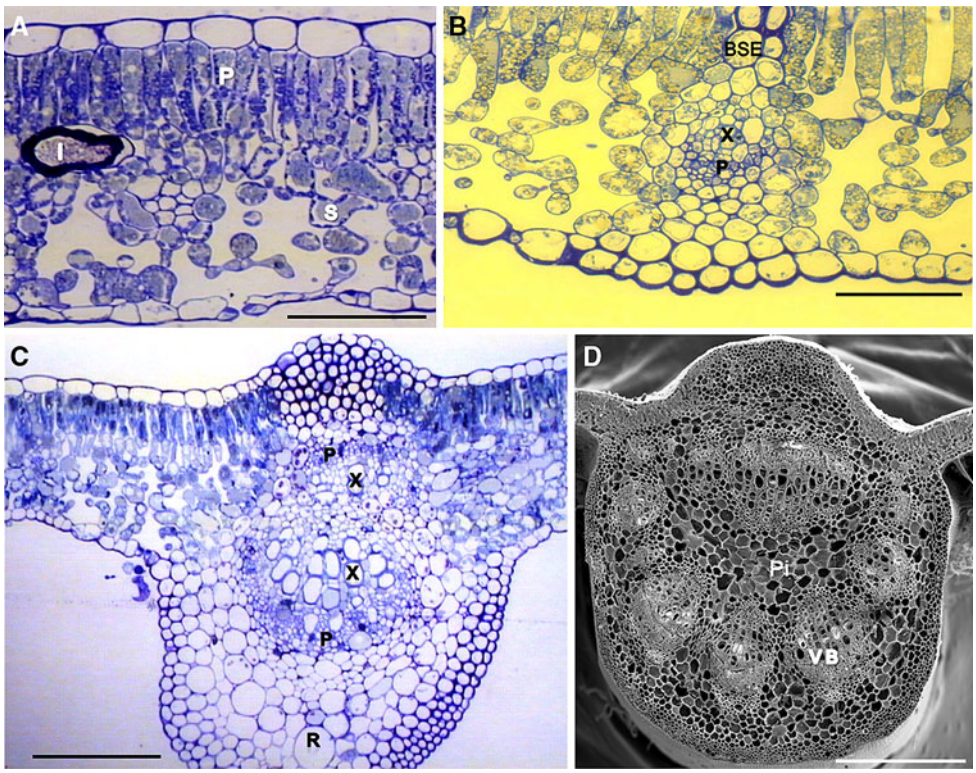

Fig. 3 Transverse sections of healthy leaves. Light micrographs of **a** epidermal cells and mesophyll cells, one of which is a large crystal-containing idioblast (*scale bar*: 100 μm), **b** a small vein showing xylem, phloem and bundle sheath extension extending towards both epidermises (*scale bar*: 100 μm), **c** vein with two vascular bundles (*scale bar*: 200 μm), and **d** SEM of the median major vein showing an open ring of surrounding pseudo-pith vascular bundles (*scale bar*: 600 μm). BSE-Bundle sheath extension, *I* Idioblast, *P* Phloem, *Pi* Pseudo-pith, *R* Rib tissue, *VB* Vascular bundle, *X* Xylem

exposed to intercellular air (Fig. 3a). The spongy parenchyma ranged from polygonal to irregularly shaped cells, some cells were isodiametric and some were elongated (Fig. 3a). The lamina also contained small veins, which were firmly anchored laterally between the palisade and spongy mesophyll cells (Fig. 3a). These intrusive veins lacked epidermal contacts and they were enclosed within a layer of compactly arranged parenchymatous bundle sheath cells. Not rarely, large oblong idioblastic cells were embedded in the mesophyll tissues (Fig. 3a). Small veins consisting of adaxially positioned xylem and abaxially positioned phloem were surrounded by parenchymatous bundle sheath cells so that the vascular tissue was rarely directly exposed to intercellular spaces (Fig. 3b). The elongated bundle sheath extensions, which are panels of cells similar to those in bundle sheaths were vertically oriented between vascular bundles and epidermises in healthy leaves and formed a vertical partition through the lamina (Fig. 3b). The bundle sheath extension cells were 2–6 cells wide and 3–6 cells in height. Some of the bundle sheath extensions were collenchymatously thickened (Fig. 3b).

A transverse section through a lateral vein with lamina and rib tissues revealed two vascular bundles, the small bundle positioned in close proximity to the adaxial surface and the large bundle just below the smaller one in the upper part of the parenchymatic rib tissues (Fig. 3c). The small bundle had adaxially-positioned primary phloem capped by a ridge of subepidermal collenchyma running along the adaxial surface and abaxially-positioned primary xylem was embedded in the parenchymatic rib tissues (Fig. 3c). In such a vascular architecture, the phloem separated the xylem vessels from the collenchymas tissue. The vascular bundles were separated from the mesophyll of the lamina by parenchyma cells (Fig. 3c). The rib surrounding the large vascular bundle extended more fully towards the marginal epidermis. The ground tissue of the rib consisted of several layers of spherical parenchyma cells of varying sizes with the smaller parenchyma cells facing the periphery towards the abaxial surface and larger cells oriented towards the vascular bundle (Fig. 3c). The walls of the peripheral rib cells and the inner walls of the epidermal cells were collenchymatously thickened (Fig. 3c).

An observation of the transverse section of the major vein of a healthy leaf with SEM revealed that the rib had a round outline (Fig. 3d). Opposite to the rib, the adaxial surface was arched and continuous with the lamina similar to the lateral veins (Fig. 3d). The vascular tissues of large major veins were arranged as a ring of separate vascular bundles of unequal size around a pseudo-pith resembling the pith in dicotyledonous stems (Fig. 3d). The vascular bundles were collateral, with outward-positioned phloem and inward-positioned xylem, as found in many dicot petioles and leaf midribs.

Leaves injured by 2,4-D were small and fan-shaped (Fig. 1b). On the adaxial surface, the lamina elevated into

several rows of bulges (blisters) of different sizes delimited by smaller veins that were confined to the depressed regions of the bulges (Fig. 4a). Such architectural alterations in the lamina conferred to the whole leaf a puckered surface (Fig. 4a). The major veins were fasciated into wide bands (Fig. 4a) whereas the small veins were crowded into depressed regions among the bulges (Fig. 4b, c). The outer epidermal cell walls extended into a ring of papillae-like structures that fit a "stonehenge" pattern; the center of the epidermal ring was depressed where the epidermal cells were polygonal with flat outer periclinal walls (Fig. 4d).

On the abaxial surface, the blisters showed a shallow to cavernous sulcus (groove) in which vein anastomozation and areolae were conspicuous (Fig. 4e–h). In these sulcuses, the epidermal cells had a similar morphology as that of epidermal cells on the adaxial surface. The trichomes took on a different orientation depending on their position in the sulcus (Fig. 4e, h). Because of hypostomaty, the interior walls of the sulcus in every plane had stomata (Figs. 4e–h, 5a). Due to a failure in positioning themselves coplanarly to the epidermal surface, some stomata of 2,4-D injured leaves in transverse sections showed the whole dimension of paired guard cells (Fig. 5b). To the author's knowledge, this is the first report in grapevine of the stomatal apparatus being situated at right angles to the epidermal plane in a transverse section.

The teeth along the leaf margins were enated into sharp projections (Fig. 5c). Each enation represented a morphed double-convex tooth of the dentate margin. The proximal ends of sinuses along the leaf margin widened forcing the teeth to project either singly, in pairs or groups that rose above the contour of the margin (Fig. 5d). At the base of

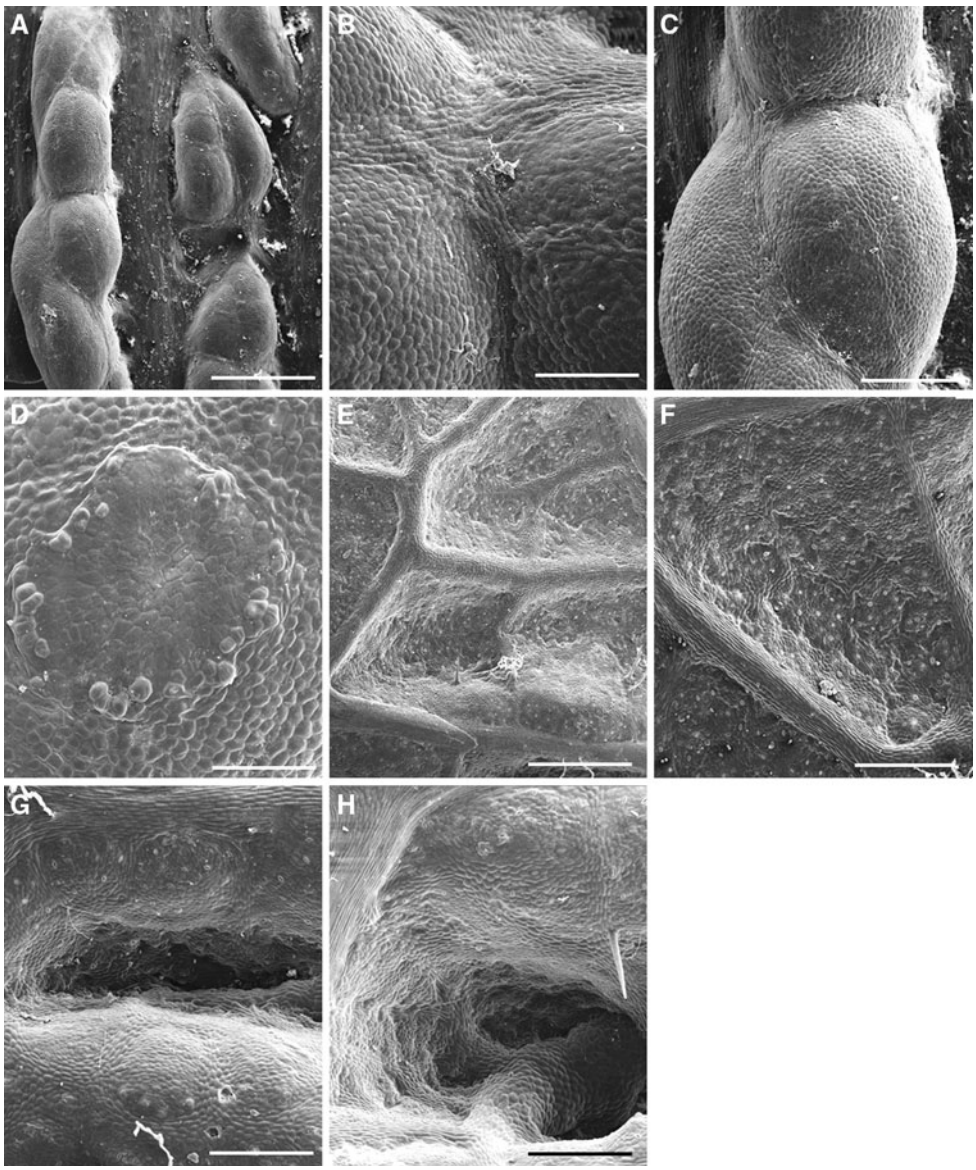

Fig. 4 Scanning electron micrographs of puckering on the adaxial surface of 2,4-D injured leaves, **a** interveinal oblong-shaped blisters (*scale bar*: 1 mm), **b** blister junction crowded with veins (*scale bar*: 176 μm), **c** veins traversing the blisters (*scale bar*: 0.38 mm), **d** annular epidermal papillae in the center of a blister (*scale bar*: 150 μm), **e** abaxial surfaces of blisters showing vein anastomozation and trichomes (*scale bar*: 0.86 mm), **f** shallow groove of a blister (*scale bar*: 0.50 mm), **g** *narrow* (scale bar: 0.30 mm) and **h** deep grooves (*scale bar*: 0.30 mm)

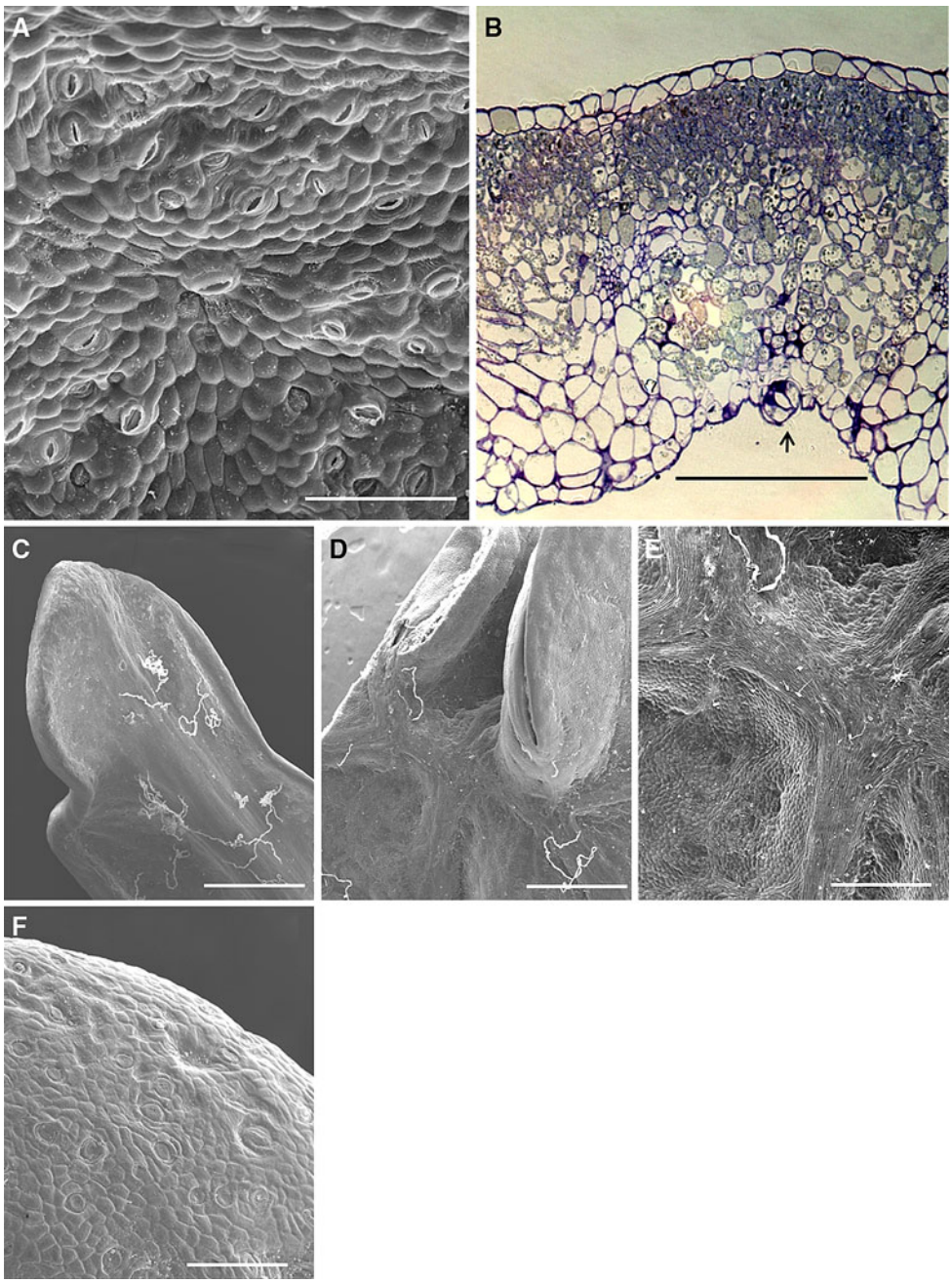

Fig. 5 Scanning electron micrograph of **a** a cluster of disoriented stomata caused by 2,4-D injury (*scale bar*: 86 μm), **b** light micrograph showing a guard cell pair (*arrow*) in a cross section of a leaf injured by 2,4-D (*scale bar*: 100 μm), **c** scanning electron micrograph of enation, single tooth (*scale bar*: 860 μm), **d** paired teeth (*scale bar*: 1000 μm), **e** fasciated and crowded veins at the proximal end of the paired teeth (*scale bar*: 430 μm), **f** malformed stomata on a leaf tooth (*scale bar*: 120 μm)

projections, the veins were crowded, tangled, and extensively fused (Fig. 5e). The stomata were sunken, poorly developed and lacked apertures (Fig. 5f). On the contrary, the teeth in lobes of healthy leaves pointed outward perpendicular to the margin with an acuminate tip (tooth) (Fig. 1a).

Scanning electron microscopy revealed a wide range of morphological alterations in stomata of 2,4-D-injured leaves (Fig. 6). Injured stomata were roundish, raised with wavy outer stomatal ledges that formed a wide outer stomatal ledge aperture with a lenticular front (outer) cavity (Fig. 6a). The guard cells were collapsed and wavy cracks and folds developed on their periclinal (dorsal) walls (Fig. 6a). Some stomata were oblong raised with blunt ends and irregular stomatal ledges (Fig. 6b), whereas in others the irregular stomatal ledges were surrounded by a flat cuticular rim (Fig. 6c). Guard cells that collapsed raised their stomatal ledges in the form of a canoe (Fig. 6d) and guard cells that became flaccid formed a rim out of their inner periphery that delimited the raised stomatal ledges, which formed a wide outer stomatal ledge aperture and a lenticular front (outer) cavity above the aperture (Fig. 6e).

Flaccidity of the guard cells rendered the stomatal pole, the axis of the stoma (aperture) where the guard cells meet, clearly visible (Fig. 6e).

In 2,4-D injured leaves, the columnar palisade parenchyma cells were modified to ovoid-shaped cells (Fig. 7a, b). On the abaxial surface, extra cell layers were formed, which consisted of rather thick-walled parenchyma cells that were separated by few or no intercellular spaces (Fig. 7a). Unlike the small veins in healthy leaves, the small veins in affected leaves were inclined at an angle between the modified palisade parenchyma cells and spongy mesophyll cells (Fig. 7c, d). The minor veins intruded on the mesophyll rather in an oblique angle and formed islets of ovoid palisade parenchyma cells (Fig. 7c, d). Because of such intrusions the vascular tissues, along with their bundle sheath cells and sheath extension, were obliquely projected through the mesophyll and became continuous with adjoining minor veins via fasciation of their bundle sheath extensions (Fig. 7c, d). The bundle sheath extensions extended upwards and downwards and contacted respective epidermal layers. The adaxial bundle sheath extension cells were 2–3 cells wide and 6–8 cells in height. The abaxial bundle sheath extensions of the two minor veins instead of individually contacting the epidermis fasciated and formed a wide ridge of collenchymatously thickened cells (Fig. 7c). Within this veinal enclosure, oval shaped palisade parenchyma cells with their elongated dimension perpendicular to the epidermal plane were densely packed with few intercellular spaces just below the epidermal cells. Thereafter, the ovoid cells interior of the lamina exhibited a loose arrangement with abundant intercellular spaces (Fig. 7b). These veinal enclosures were roofed above and below by epidermal layers (Fig. 7c, d). Crystal-containing idioblasts were often found embedded in the mesophyll tissues near the palisade-spongy interface.

The epidermal cells of 2,4-D inured leaves were not tabular on either surface (Fig. 7). Within each epidermis, there was a remarkable size difference among epidermal

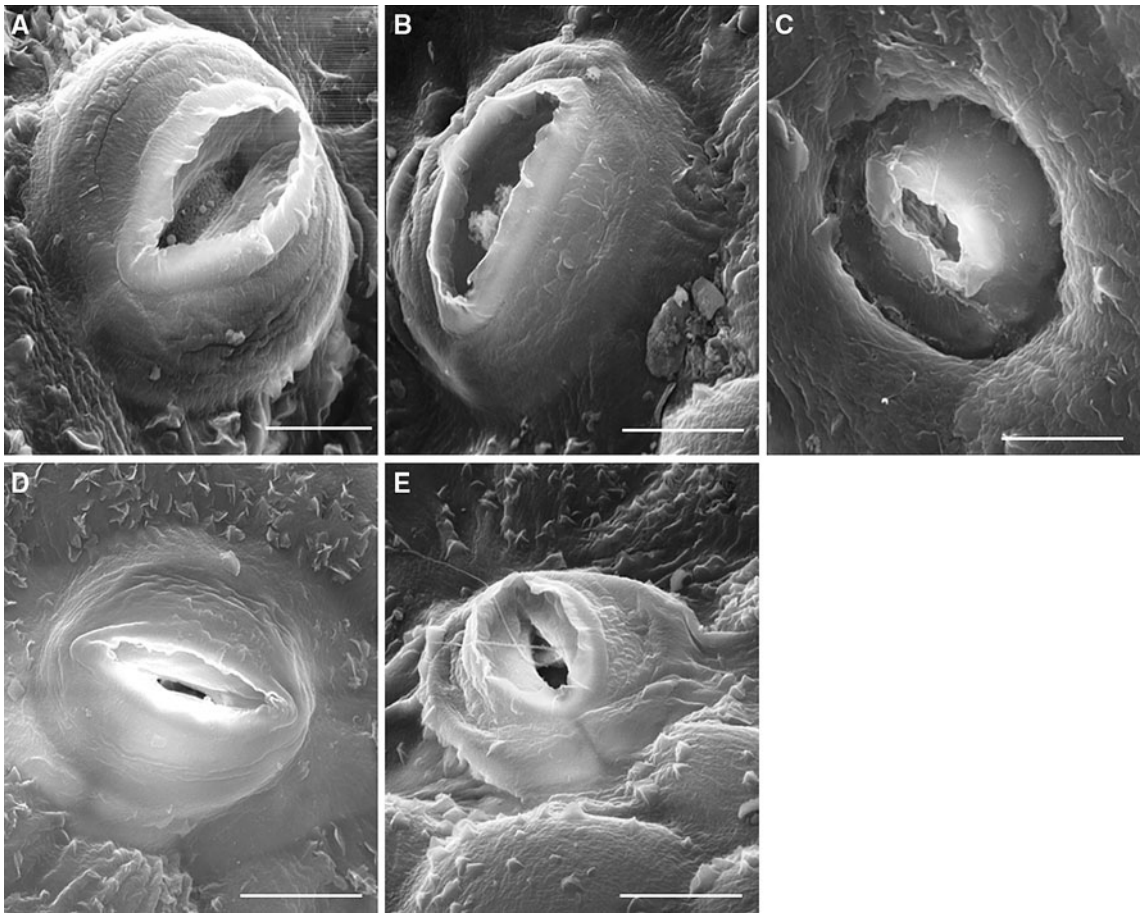

Fig. 6 Scanning electron micrographs of stomata injured by 2,4-D, **a** round raised stoma with cracks on guard cells and wavy stomatal ledges and, **b** stoma surrounded by thick cuticular rim with wavy stomatal ledges, **c** collapsed guard cells with canoe shaped stomatal ledges, **d** flaccid guard cells with raised stomatal ledges, and **e** flaccidity of guard cells displaying a rim formation from their inner periphery and the stomatal pole, i.e. the axis of the stoma to be clearly visible. Scale bars: 10 μm (**a**), 7.5 μm (**b**), and 12 μm (**c**, **d**, and **e**)

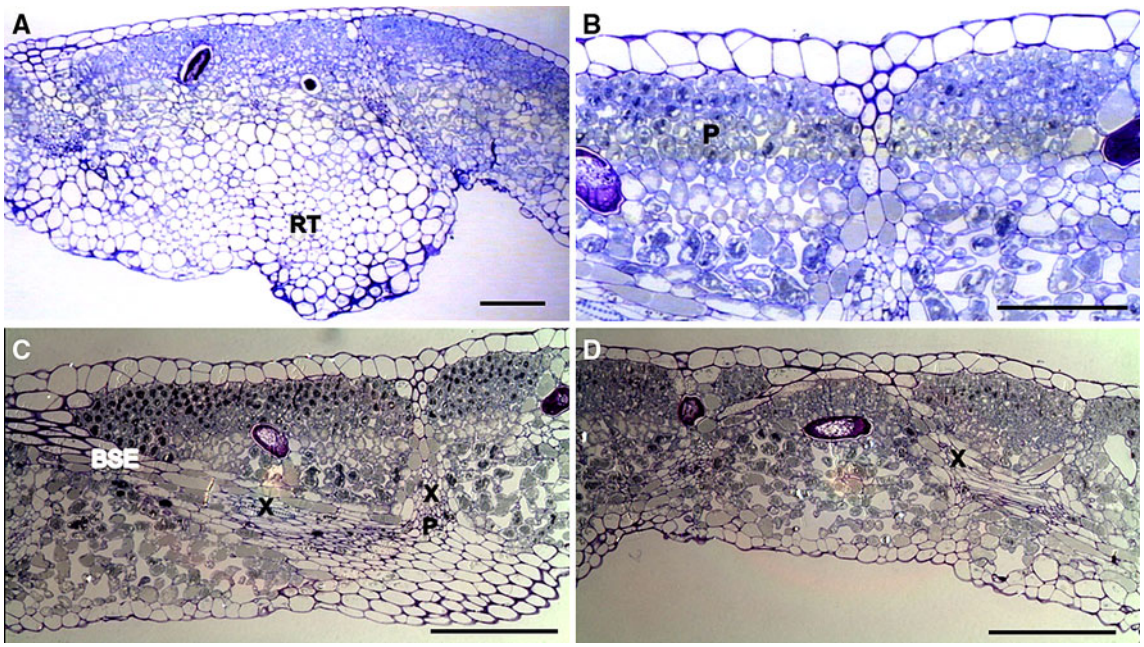

Fig. 7 Light micrographs showing transverse sections of leaves injured by 2,4-D. **a** Altered mesophyll cells and replacement tissues (*scale bar*: 100 μm), **b** ovoidal palisade parenchyma cells with intercellular spaces (*scale bar*: 100 μm), **c** lower magnification of B, showing bundle sheath extension (BSE) intruding on the mesophyll in an oblique angle and forming islets of ovoid palisade parenchyma cells (*scale bar*: 200 μm), and **d** bundle sheath extensions (BSE) of two adjacent intrusive veins running diagonally through the mesophyll tissues and uniting sub-epidermally towards the adaxial surface (*scale bar*: 200 μm). *BSE* Bundle sheath extension, *P* Parenchyma cells, *Ph* Phloem, *RT* Replacement tissue, *X* Xylem

cells; however, most of them were elongated anticlinally protruding either inward or outward and thus did not lie on the epidermal plane (Fig. 7b). Similar to healthy leaves, the outer and inward facing cell walls were convex with the outer walls being thicker than the inner walls due to cuticular deposits (Fig. 7). Occasionally, there was a space in the adjoining area between the inward facing cell walls and the chlorenchyma cells. Unlike in healthy leaves, the epidermal cells in affected leaves were not aligned linearly, they appeared to be piled up on one another reminiscent of a multiple epidermis (Fig. 7c, d). The plane of attachment (anticlinal walls) between two epidermal cells was slanted with varying angles.

Fasciation of two or more major veins (vascular bundles including the ground tissue) in one plane produced the flattening effect of "riband-fasciation" (like a ribbon) transforming their radial symmetry to bilateral symmetry (Fig. 8). Along the plane of fusion, deep V-shaped grooves existed that were prominent on the abaxial surfaces and the periphery on the abaxial surface had a wavy outline (Fig. 8). In the fasciated veins, the ground tissues of one vein became continuous with the adjoining vein, hence their cross sectional area was greater than non-fasciated veins in the healthy leaves. A separate ring of vascular bundles existed in each vein, although it was flattened (Fig. 9a, c, e). Because of flattening, the vascular bundles became laterally arranged parallel to the adaxial and abaxial surfaces of the vein. Just as the fasciated veins as a whole differed from the cylindrical shape, so did the individual tissues (Fig. 9). The epidermis, parenchyma and collenchymas cells, and the vascular tissues conformed in outline to the general shape of the vein. Among all the tissues, the most distorted were the pseudo-pith parenchyma cells and the xylem (Fig. 9b, d, f), these tissues, therefore may be spoken of individually as fasciated tissues. Similar features were observed when smaller lateral veins fasciated except that they had raised lamina between them (Fig. 8d).

Discussion

As expected, 2,4-D injury free leaves were flattened, which is usually the first morphological indication of dorsiventral polarity within the leaves (Pratt 1974) and results from rapid cell division along the margins during development from leaf primordia (McConnell and Barton 1998). This type of asymmetry in any leaf generally reflects the functioning of adaxial surfaces in optimizing light capture for photosynthesis and the abaxial surfaces in developing the necessary pathways for gas exchange (Aalto and others 1999; Tasaka 2001). Furthermore, the unequal apportioning of chloroplasts between mesophyll cells is considered

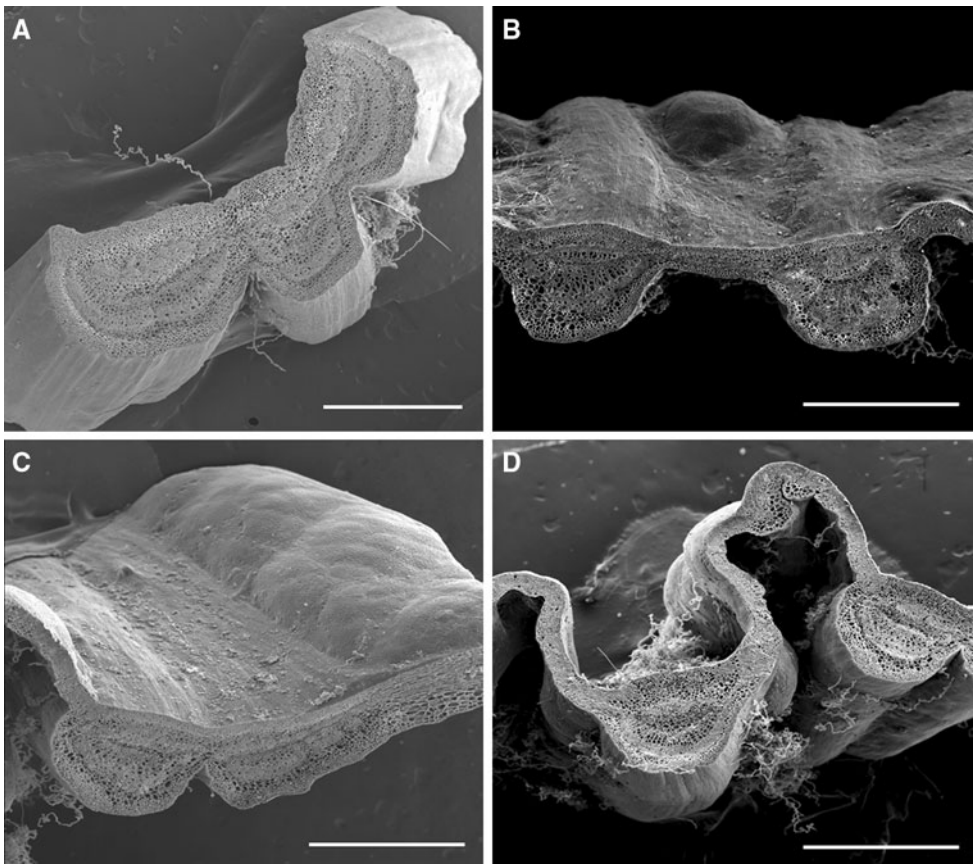

Fig. 8 Scanning electron micrographs of fasciated veins from 2,4-D injured leaves, **a** three fasciated veins with no interveinal lamina, **b** two fasciated veins with small interveinal lamina, **c** two fasciated veins with no interveinal lamina, and **d** two fasciated major veins with interveinal lamina showing fasciation of small veins. *Scale bars*: 860 μm (**a**–**c**), 1 mm (**d**)

to be an adaptation to the higher fluence rates for photosynthetically active radiation generally incident on the adaxial surfaces of the leaf (Niinemets and others 2004). This explains why in a bifacial leaf (for example, grapevine leaf), the photosynthetic activity of palisade parenchyma cells generally dominates over spongy mesophyll cells (Bondada and others 1994; Mott 2009). In terms of volume, the palisade parenchyma accounted for almost 50% of the leaf thickness; however, it varied in other *Vitis* spp. from just a third (*V. rupestris*) to half (*V. riparia*, *V. lubrasca*), to more than half (*V. vulpina*) of the thickness (Wylie 1939). The palisade layer also housed idioblasts with crystals of calcium oxalate in contrast with a study by Bernard (1971) who reported idioblasts throughout the leaf blade. What advantages idioblasts offer to leaves are not known; however, when restricted to the palisade cells, they have been implicated in dispersing light to chloroplasts (Kuo-Huang and others 2007).

As opposed to healthy leaves, the 2,4-D injured leaves developed rugose bands of lamina, which is a classic 2,4-D injury symptom in grapevine leaves that have absorbed 2,4-D either from drift or foliar sprays (Bondada and others 2006). Other crops such as beans (Watson 1948) and *Datura stramonium* L. (Wassberg and Goodrich 1956) also developed a similar morphology in response to 2,4-D. Translocated primarily in the phloem, 2,4-D accumulates in the meristematic regions (Teixeira and others 2007). Accordingly the altered morphology involving rugose bands of lamina arose from the loss of structural integrity of meristematic cells in this region, especially the intercalary meristem responsible for promoting blade expansion in grapevine leaves (Pratt 1974). Consequently, the perturbed functions of the intercalary meristem led to uneven and disorganized growth of various cell layers in the interveinal lamina, which was primarily composed of ovoid parenchyma cells similar to the ones observed in apricot leaves affected by the 2,4-D analog 2,4, 5-T (2,4,5-trichlorophenoxyacetic acid) (Bradley and others 1968). Given that the palisade parenchyma originates from plate meristem established by the activities of the marginal meristem (McConell and Barton 1998), the morphed palisade parenchyma reflected an aberrant plate meristem induced by the action of 2,4-D in injured leaves. Furthermore, the bundle sheath extensions (BSE) bordering the islets of these morphed cells shifted to an oblique angle. In healthy grapevine leaves, the BSE in vertical orientation act as transparent windows and enrich the neighboring mesophyll areas with high levels of photosynthetically active radiation (Karabourniotis and others 2000). Whether or not the distorted arrangement of BSE in 2,4-D injured

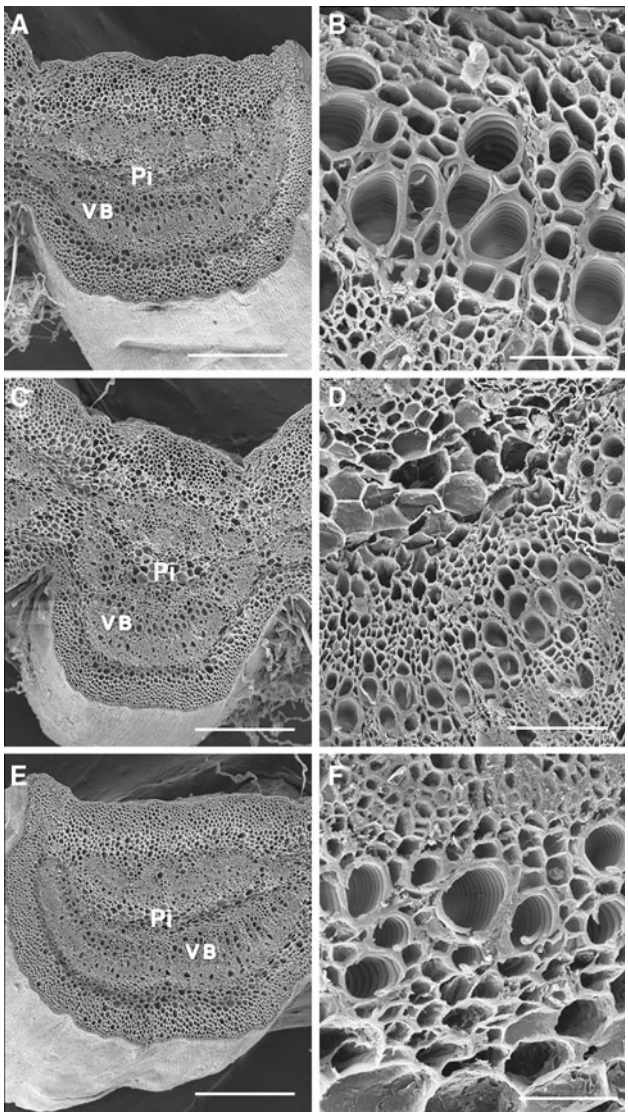

Fig. 9 Greater details of scanning electron micrographs of the right-hand (**a, b**), middle (**c, d**), and left-hand (**e, f**) fasciated veins seen in Fig. 8a. (**a**, **c**, and **e**) Thickened ribs and general flattening of the vascular ring; (**b**, **d**, and **f**) magnified views of vascular anatomy, especially the scalariform vessel elements. *Scale bars*: **a** and **c** 380 μm, **b** 100 μm, **d** and **f** 38 μm, **e** 380 μm. *Pi* Psuedo-pith, *VB* Vascular bundle

leaves affected its light-transferring function could not be ascertained from this study as the light gradients along the BSE and mesophyll were not monitored. The sub-palisadal layers in these sections failed to develop abundant intercellular spaces in the spongy mesophyll cells analogous to glyphosate action in *Eucalyptus* leaves; however, glyphosate did not alter anatomy of the mesophyll cells (Santos and others 2009). Idioblasts also occurred in the palisade cells, whether or not 2,4-D affected idioblasts ontogeny or function could not be determined from their structure. On the other hand, it reduced the amount of calcium oxalate crystals in *Datura stromonium* (Wassberg and Goodrich 1956).

These structural modifications in the mesophyll cells of 2,4-D injured leaves have severe consequences for photosynthesis. For instance, substantial spaces among palisade cells cause desiccation of leaves especially under limited water conditions and a lack of intercellular spaces in the spongy mesophyll cells reduces gas exchange (Poulson and Vogelmann1990). Stomatal functioning is perturbed as signals from mesophyll cells (palisade parenchyma) regulate stomatal responses to light and CO_2 (Mott 2009). Furthermore, loss of tubular shape of palisade parenchyma cells impedes light penetration and vertical placement of chloroplasts optimal for photosynthesis (Vogelmann and Martin 1993). More specifically, 2,4-D has been reported to inhibit photosynthesis by damaging membrane systems of the mesophyll cells (Loustalot and Muzik 1953; Romero-Puertas and others 2004) and distorting chloroplast ultrastructure (Hallam 1970; Romero-Puertas and others 2004) indicating mesophyll cells, in particular the chloroplasts as the site of 2,4-D accumulation (Hallam and Sargent 1970).

Although 2,4-D injured leaves maintained dorsiventral polarity together with adaxial-abaxial patterns of cellular structure and composition, extra cell layers originating in the spongy mesophyll proliferated near the abaxial leaf surface. This new tissue was analogous to tissues observed in 2,4-D injured cotton (Gifford 1953). However, in bean plants, the extra cell layers transformed into protuberances of different patterns (Felber 1948; Watson 1948). These extra cell layers have been identified as "replacement tissue" (Dickison 2000). Taken together, these findings lead to a consensus view that one of the striking responses of different plant species to 2,4-D is the tendency of cells to become meristematic, which apparently disrupts the orderly metabolical and physiological processes and thus leads to nonpolarized cell division and abnormal growth patterns.

The deviation of epidermal layers from horizontal assemblages of cells partly accounts for the failure of the lamina to fully expand. This reasoning is based on a recent study entailing the crucial role of the epidermis in blade expansion and final leaf size (Marcotrigiano 2010) through its involvement with growth-promoting plant hormones called brassinosteroids (Scheres 2007; Savaldi-Goldstein and others 2007). The aggregated epidermal cells appeared to be a distinctive feature of 2,4-D injured grapevine leaves. In other crops, by contrast, 2,4-D stimulated epidermal cells to develop a tetragonal shape as in *Datura stramonium* (Wassberg and Goodrich 1956), enlarged them in grass and pea leaves (Eames 1949), and collapsed their membrane systems in bean plants (Hallam 1970; Romero-Puertas and others 2004). Although the symptoms varied in response to 2,4-D, altogether, these abnormalities in

epidermal cells were evident of major perturbations in the activity of plate meristems whose function was altered differentially depending upon plant species. In contrast, the healthy leaves not only had epidermal cells on the epidermal plane, but also they were convex, which captures maximum incident light for utilization by the underlying photosynthetic tissues than cells of any other shape (Poulson and Vogelmann (1990).

Because epidermal cells control stomatal development and apertures (Nadeau and Sack 2002), the crowding and piling up of epidermal cells in 2,4-D injured leaves contributed to the displacement of the stomata from the epidermal plane. However, the distorted and flaccid guard cells with anomalous stomatal ledges were direct evidence of 2,4-D inhibiting metabolic reactions required to maintain guard cell turgor. These extreme modifications in stomata did not occur in other species, for instance, in *Datura stramonium*, the stomata elongated longitudinally (Wassberg and Goodrich 1956) whereas in kidney bean plants, stomatal closure was observed without any damage to guard cells, which usually is the case in the event of 2,4-D exposure (Bradbury and Ennis 1952). Other mechanisms of 2,4-D injury to stomata entailed altered membrane permeability and inhibited accumulation of potassium (Pemadasa and Jeyaseelan 1976). Grapevines or any plant with the aforementioned stomatal anomalies will sustain impaired plant growth and yield because stomata control the entry of carbon dioxide assimilated in photosynthesis and optimize water use efficiency (Roelfsema and Hedrich 2005). As opposed to stomata, the epicuticular wax in the form of platelets was similar to that seen in healthy leaves. These platelets are the most common crystalloids of the leaf epidermis and are found in all major plant groups: mosses, ferns, gymnosperms and angiosperms and act as barriers to foliar-applied chemicals and cuticular transpiration (Bondada and others 1996; Bartholtt and others 1998; Bondada and others 2006).

A conspicuous feature of 2,4-D injury in grapevine leaves was fasciation of veins, which was also observed in response to the growth regulator morphactin (Weaver and Pool 1971). Fasciation refers to teratological (developmental) abnormality, a genetically determined and rather widespread mutation in the plant world (White 1948). It involves fusion of the tissues or plant organs, which, as a whole or in part generates a flat, banded, or ribbon shape (Sinjushin and Gostimski 2008). As the major veins provide hydraulic supply (Sack and others 2008), the fasciation of veins of grapevine leaves might have disrupted the rapid delivery of water and solutes to the whole length of the lamina. Factors other than herbicides and growth regulators that induce fasciation include various infections, traumas or amputation of the apical meristem, deficiency of micronutrients, and so on (Sinjushin and Gostimski 2008). Although only the veins of grapevine leaf fasciated, varied fasciation patterns have been observed in species other than grape. For instance, 2,4-D caused leaf fusion and contortion in Marigold (Holly 1954) and funnel leaf in spinach (Kendrick and Middleton 1954). Evidently, 2,4-D triggers fasciation of plant parts, but how it does so is not known. Nonetheless, in one study an inhibitor of auxin transport was correlated with stem fasciation (Gorter 1965). In relation to internal tissues of grapevine leaves, 2,4-D-induced fasciation distorted the pith parenchyma cells and the xylem. Phloem as a whole was identifiable in the light and SEM micrographs, whether or not 2,4-D caused damage to phloem cells was not recognizable for two reasons. Firstly, phloem tissues are typically surrounded by other vascular and support tissues associated with leaf veins, which in turn are embedded in the mesophyll, hence in transverse sections the sieve tubes and phloem parenchyma cells look alike (Milburn and Kallarackal 1983; Esau 1947). Secondly, phloem morphology and its cell constituents are generally resolved using transmission electron microscopy (for example, Turgeon and others 2001). In view of the fact that the present study was conducted at the histological level, no attempt was made to determine injury to phloem cells. Even though phloem damage was not recognizable from our study, 2,4-D has been shown to destroy phloem cells, for instance, in hypocotyl of bean plants (Eames 1950).

In conclusion, the 2,4-D injured leaves of grapevine showed severe abnormalities in their external and internal organization of cells. The epidermal cells in 2,4-D injured leaves lacked tabular structure; they were clumped together and hence, did not lie solely on the epidermal plane. The guard cells of stomata were flaccid and collapsed, developed wrinkles with irregular stomatal ledges; most importantly their position was disoriented. The mesophyll consisted of ovoidal palisade parenchyma cells with intercellular spaces, less porous spongy mesophyll tissues, and replacement tissues in the spongy region. The major and minor vein systems were fasciated resulting in the fasciation of internal tissues. These internal structural modifications produced gross morphological changes manifested as enations at leaf margins and interveinal puckering of lamina. Unequivocally, leaves developing such anatomical and morphological alterations may lose their inherent capacity to photosynthesize sugars and transpire water leading to senescence and necrosis ultimately causing plant death, which therefore, at least in part can be attributed to injured leaves.

Acknowledgment The author thanks Dr. Valerie Lynch of School of Biological Sciences for her technical assistance.

References

Aalto T, Vesala T, Mattila T, Siemborowicz P, Hari P (1999) A three-dimensional stomatal CO_2 exchange model including gaseous phase and leaf mesophyll separated by irregular interface. J Theor Biol 196:115–128

Al-Khatib K, Parker R, Fuerst P (1991) Wine grape (*Vitis vinifera* L.) response to simulated herbicide drift. Weed Tech 7:97–102

Bartholtt WC, Neinhuis D, Cutler F, Ditsch I, Meusel I, Wilhelmi H (1998) Classification and terminology of plant epicuticular waxes. Bot J Linn Soc 126:237–260

Bernard AC (1971) L'oxalate de calcium chez la vigne. La France Viticole 6:149–155

Bhatti MA, Al-Khatib K, Parker R (1996) Wine grape (*Vitis vinifera*) response to repeated exposure of selected sulfonylurea herbicides and 2,4-D. Weed Tech 10:951–956

Bondada BR, Oosterhuis DM, Wullschleger SD, Kim KS, Harris WM (1994) Anatomical considerations related to photosynthesis in cotton leaves, bracts, and the capsule wall. J Exp Bot 45:111–118

Bondada BR, Oosterhuis DM, Murphy JB, Kim KS (1996) Effect of water stress on the epicuticular wax composition and ultrastructure of cotton leaf, bract, and boll. Env Exp Bot 36:61–69

Bondada BR, Hebert V, Keller M (2006) Morphology, anatomy, and ultrastructure of grapevine (*Vitis vinifera* L.) leaves injured by 2,4-D. Botanical Society of America, 26 July–2 Aug, Chico, CA. Abstr 241, p 111

Bradbury D, Ennis WB Jr (1952) Stomatal closure in kidney Bean plants treated with ammonium 2,4-Dichlorophenoxy acetic acid. Am J Bot 39:324–328

Bradley MV, Crane JC, Marei N (1968) Some histological aspects of 2,4,5-trichlorophenoxyaceticacid applied to mature apricot leaves. Bot Gaz 129:231–238

Dickison WC (2000) Integrative plant anatomy. Academic Press, San Diego

Eames AJ (1949) Comparative effects of spray treatments with growth-regulating substances on the Nut Grass, *Cyprus rotundus* L., and anatomical modifications following treatment with Butyl 2,4-Dichlorophenoxyacetate. Amer J Bot 36:571–584

Eames AJ (1950) Destruction of phloem in young bean plants after treatment with 2,4-D. Amer J Bot 37:840–847

Esau K (1947) A study of some sieve-tube inclusions. Amer J Bot 34:224–233

Felber IM (1948) The formation of protuberances on bean leaves in response to 2,4-D treatments. Amer J Bot 35:555–558

Gifford EM (1953) Effect of 2,4-D upon the development of the cotton leaf. Hilgardia 21:605–644

Gorter CJ (1965) Origin of fasciation. In: Ruhland W (ed) Encyclopedia of plant physiology. Springler-Verlag, New York, pp 330–351

]Grossmann K (2000) Mode of action of auxin herbicides: a new ending to a long, drawn out story. Trends Plant Sci 5:506–508

Hallam (1970) The Effect of 2,4-Dichlorophenoxyacetic acid and related compounds on the fine structure of the primary Leaves of Phaseolus vulgaris. J Exp Bot 21:1031–1038

Hallam ND, Sargent JA (1970) The localization of 2,4-D in leaf tissues. Planta 94:291–295

Holly K (1954) Morphological effects on plants due to damage by growth-regulator weed killers. Plant Path 3:1–5

Horiguchi G, Fujikura U, Ferjani A, Ishikawa N, Tsukaya H (2006) Large-scale istological analysis of leaf mutants using two simple leaf observation methods: identification of novel genetic pathways governing the size and shape of leaves. Plant J 48:638–644

Karabourniotis G, Bornman JF, Nikolopoulos (2000) A possible optical role of the bundle sheath extensions of the heteroblastic leaves of *Vitis vinifera* and *Quercus coccifera*. Plant Cell Environ 23:423–430

Kasimatis AN, Weaver J, Pool RM (1968) Effects of 2,4-D and 2,4-DB on the vegetative development of 'Tokay' Grapevines. Amer J Vit Enol 19:194–204

Kendrick JB Jr, Middleton JT (1954) Funnel-leaf of spinach induced by 2,4-D. Bulletin torrey bot. Club 2:137–140

Kuo-Huang LL, Ku MSB, Franceschi VR (2007) Correlations between calcium oxlate crystals and photosynthetic activities in palisade cells of shade adapted *Peperomia glabella*. Bot Stud 48:155–164

Kust CA, Struckmeyer BE (1971) Effects of trifluralin on growth, nodulation, and anatomy of soybeans. Weed Sci 19:147–152

Loustalot AJ, Muzik TJ (1953) Effect of 2,4-D on apparent photosynthesis and developmental morphology of velvet bean. Bot Gaz 115:56–66

Marcotrigiano M (2010) A role for leaf epidermis in the control of leaf size and the rate and extent of mesophyll cell division. Amer J Bot 97:224–233

McConell JR, Barton MK (1998) Leaf polarity and meristem formation in *Arabidopsis*. Development 125:2935–2942

Milburn JA, Kallarackal J (1983) Quantitative determination of sieve-tube dimensions in *Ricinus*, *Cucumis* and *Musa*. New Phytol 96:383–395

Mott K (2009) Opinion: stomatal response to light and CO_2 depend on mesophyll. Plant Cell Environ 32:1479–1486

Mullins MG, Bouquet A, Williams LE (1998) Biology of the grapevine. Cambridge University Press, Melbourne

Nadeau JA, Sack FD (2002) Control of stomatal distribution on the *Arabidopsis* leaf surface. Science 296:1697–1700

Niinemets U, Tenhunen JD, Beyschlag W (2004) Spatial and age dependent modifications of photosynthetic capacity in four Mediterranean oak species. Func Plant Biol 31:1179–1193

Pemadasa A, Jeyaseelan K (1976) Some effects of three herbicidal auxins on stomatal movements. New Phytol 77:569–573

Poulson MET, Vogelmann C (1990) Epidermal focusing and effects on photosynthetic light-harvesting in leaves of Oxalis. Plant Cell Environ 13:803–811

Pratt C (1974) Vegetative anatomy of cultivated grapes–a review. Amer J Enol Vit 25:131–150

Roelfsema MR, Hedrich R (2005) In the light of stomatal opening: new insights into 'the Watergate'. New Phytol 167:665–691

Romero-Puertas MC, Gomez MM, Sandalio LM, Corpas FJ, Del Rio LA, Palma JM (2004) Reactive oxygen species-mediated enzymatic systems involved in the oxidative action of 2,4-dichlorophenoxyacetic acid. Plant Cell Environ 27:1135–1148

Sack L, Dietrich EM, Streeter CM, Sanchez-Gomez D, Holbrook NM (2008) Leaf palmate venation and vascular redundancy confer tolerance of hydraulic disruption. Proc Nat Acad Sci 5:1567–1572

Santos T, Sant'Anna-Santos LD, Meira BF, Ferreira RMSA, Tiburcio FA, Machado AFL (2009) Leaf anatomy and morphometry in three eucalypt clones treated with glyphosate. Braz J Biol 69:129–136

Savaldi-Goldstein S, Peto C, Chory J (2007) The epidermis both drives and restricts plant shoot growth. Nature 446:199–202

Scheres B (2007) The force from without. Nature 446:151–152

Sciumbato AS, Chandler JM, Senseman SA, Bovey RW, Smith KL (2004) Determining exposure to auxin-like herbicides: I. Quantifying injury to cotton and soybean. Weed Techn 18:1125–1134

Sinjushin AA, Gostimski SA (2008) Genetic control of fasciation in pea (*Pisum sativa* L). Russian J Genet 44:702–708

Skirvin R (2008) Biologist creates herbicide-resistant grape. Wine & Vines December issue, 64

Tasaka M (2001) From central-peripheral to adaxial to abaxial. Trends Plant Sci 6:548–550

Teixeira MC, Duque P, Sa-Correia I (2007) Environmnetal genomics: mechanistic insights into toxicity of and resistance to the herbicide 2,4-D. Trends Biotech 25:363–370

Tukey HB (1947) 2,4-D, a potent growth regulator of plants. The Sci monthly 64:93–97

Turgeon R, Medville R, Nixon KC (2001) The evolution of minor vein phloem and phloem loading. Amer J Bot 88:1331–1339

Vogelmann TC, Martin G (1993) The functional significance of palisade tissue: penetration of directional versus diffuse light. Plant Cell Envirn 16:65–72

Wassberg C, Goodrich FJ (1956) A study on the anatomical effects produced in the leaves of *Datura stramonium* L. by the action of 2,4-Dichlorophenoxy acetic acid. J Amer Pharm Assoc 45:495–497

Watson DP (1948) An anatomical study of the modification of bean leaves as a result of treatment with 2,4-D. Amer J Bot 35:543–555

Weaver R, Pool RM (1971) Effect of succinic acid-2,2-Dimethylhydrazide and (2-Chloroethyl) trimethylammonium chloride on shoot growth of 'Tokay' Grapes. Am J Enol Vitic 22:223–226

Weintraub R (1953) 2,4-D, Mechanism of action. Agric Food Chem 1:250–254

White OE (1948) Fasciation. Bot Rev 14:319–358

Wylie RB (1939) Relationship between tissue organization and vein distribution in dicotyledon leaves. Amer J Bot 26:219–225